

Article

Numerical Stability Investigations of the Method of Fundamental Solutions Applied to Wave-Current Interactions Using Generating-Absorbing Boundary Conditions

Mohammed Loukili ¹, Denys Dutykh ^{2,*}, Kamila Kotrasova ³ and Dezhi Ning ¹

¹ State Key Laboratory of Coastal and Offshore Engineering, Dalian University of Technology, Dalian 116023, China; md.loukili@gmail.com (M.L.); dzning@dlut.edu.cn (D.N.)

² Univ. Grenoble Alpes, Univ. Savoie Mont Blanc, CNRS, LAMA, 73000 Chambéry, France

³ Faculty of Civil Engineering, Technical University of Kosice, Vysokoškolská 4, 042 00 Košice, Slovakia; kamila.kotrasova@tuke.sk

* Correspondence: Denys.Dutykh@univ-smb.fr

Abstract: In this paper, the goal is to revolve around discussing the stability of the Method of Fundamental Solutions (MFS) for the use case of wave-current interactions. Further, the reliability of Generating-Absorbing Boundary Conditions (GABCs) applied to the wave-current interactions is investigated using the Method of Fundamental Solutions (MFS), in a Numerical Wave Tank (NWT) within the potential theory where the main regular manifestations are the periodicity, and symmetry of traveling waves. Besides, the investigations cover different aspects of currents (coplanar current, without current, and opposing current), and also different water depths. Furthermore, the accuracy and stability of the numerical method (MFS) used in this work is evaluated for different locations and numbers of source points.



Citation: Loukili, M.; Dutykh, D.; Kotrasova, K.; Ning, D. Numerical Stability Investigations of the Method of Fundamental Solutions Applied to Wave-Current Interactions Using Generating-Absorbing Boundary Conditions. *Symmetry* **2021**, *13*, 1153. <https://doi.org/10.3390/sym13071153>

Academic Editor: Rahmat Ellahi

Received: 20 May 2021
Accepted: 25 June 2021
Published: 27 June 2021

Publisher's Note: MDPI stays neutral with regard to jurisdictional claims in published maps and institutional affiliations.



Copyright: © 2021 by the authors. Licensee MDPI, Basel, Switzerland. This article is an open access article distributed under the terms and conditions of the Creative Commons Attribution (CC BY) license (<https://creativecommons.org/licenses/by/4.0/>).

Keywords: MFS method; GABCs; wave-current interactions; numerical wave tank

1. Introduction

In marine and coastal environments, harmonic waves' profiles are generally periodic and symmetric as soon as the wave is monotone between successive crests and troughs. Even more, the waves are mostly paired with currents, which are generated by a variety of mechanisms, such as readily observed when density currents develop in estuaries and inlets due to the interaction of freshwater from riverine run-off with more dense saline water from the surrounding coastal environment. Further, waves in the ocean environment usually coexist with various currents, including tidal currents and wind-driven currents. In the same context, the computational simulations of wave-current interactions play a significant role in collecting and estimate nautical data for the use of protection, operations (surface and submarine), and other marine activities. For these reasons, coastal engineers and researchers have devoted considerable attention to the significance of the numerical study of wave-current interactions for various facets of maritime operations. Especially, the precise choice of appropriate and feasible boundary conditions is most interesting topic to should shed light on it. Further, the use of effective boundary conditions in coastal engineering are revolved around accurate resolutions of many problems such as the excellence numerical measures of reflections and transmissions due to wave-structure interactions.

Shedding light on the latest state-of-the-art, Manolidis [1] has studied rogue wave formation in adverse ocean current gradients using computational fluid dynamics (CFD). Wave propagation over a submerged breakwater in the presence of a steady current was studied experimentally and numerically by Chen [2]. Likewise, Lin [3] has studied wave-plate-current interactions using a higher-order boundary element method. In [4] the local radial point interpolation collocation method (LRPICM) is used to study the nonlinear

wave–wave and wave–current interactions in the time domain. Besides, in the [5,6] the smoothed-particle hydrodynamics (SPH) method is used to study wave-current interactions. Zhang [7] has developed a numerical model to study the wave-current interactions based on the Reynolds-averaged Navier–Stokes (RANS) model. Fan and Zhang [8,9] investigated wave-current interactions and wave-structure interactions using a finite difference method. Several studies on numerical waves, wave-structure interactions, and wave-current interactions have been conducted where sponge conditions have been used. However, for certain practical situations such as truncated domains, the sponge layer boundary condition is not efficient. Further, a series of computational experiments are necessary to challenge deciding the optimum parameters. For these reasons, the generating-absorbing boundary conditions (GABCs) in the presence of different aspect of currents (coplanar current, opposing current, and without current) is an interesting subject to investigate. Therefore, in this work the generating absorbing boundary conditions (GABCs) for the use of wave-current interactions is studied using the method of fundamental solutions (MFS) [10–13]. The MFS first proposed by Kupradze and Aleksidze [14] and has been widely used in the numerical solutions for the Laplace, Poisson, biharmonic, Helmholtz and diffusion equations. Mathon and Johnston [15] used the MFS to numerically solve the elliptic boundary value problems. It is also used to study Stokes equations [16], Navier-Stokes equations [17], Helmholtz and diffusion problems [18], Biharmonic equation [19]. MFS always appears as a powerful numerical method in dealing with linear and nonlinear problems [10–13,20,21].

In this work, the intention is to discuss the capacity and stability, and the efficiency of GABCs applied to the wave-current interactions using the MFS, in a numerical wave tank (NWT) within the potential theory where the concept of symmetry plays an essential role to define traveling waves. Likewise, the stability investigations of the numerical method (MFS) is evaluated for different locations and numbers of source points. Furthermore, these investigations are presented for different aspects of currents (coplanar current, without current, and opposing current). Besides, the GABCs will be evaluated for different water depths.

This paper is divided into five main sections. After introducing the goal of this research in the Section 1, the problem statement of this work and the numerical method used are clearly presented in the Section 2 and 3. In the Section 4, the numerical results, comparisons, and analysis are presented to confirm and ensure the capacity and stability of the MFS and the GABCs to treat the wave-current interactions. Finally, conclusions and perspectives are illustrated in the Section 5.

2. Problem Statement

In this paper, the fluid is presumed to be incompressible, irrotational and inviscid, as well as the symmetry of wave profiles is necessary to define traveling waves. Further, we consider a steady current U along the x -direction in interaction with waves in a NWT as illustrated in Figure 1.

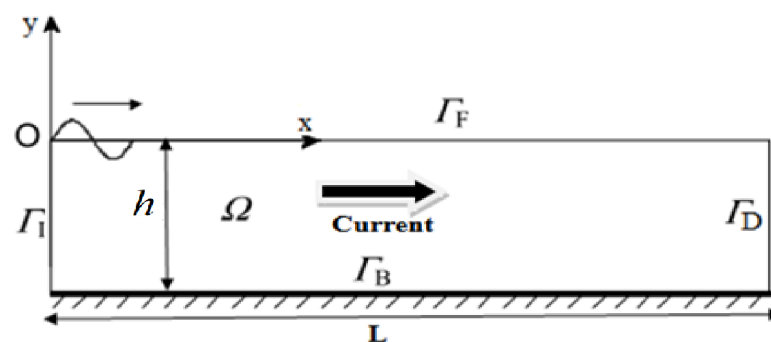


Figure 1. Sketch of NWT in the presence of current.

Within the potential theory, the equations govern the problem of linear wave-current interactions, are written as:

$$\Delta\phi_w = 0 \text{ in } \Omega, \quad (1)$$

$$\frac{\partial\phi_w}{\partial y} = 0 \text{ in } \Gamma_B, \quad (2)$$

$$\frac{\partial\phi_w}{\partial t} + g\eta + \frac{1}{2}\left(U^2 + 2U\frac{\partial\phi_w}{\partial x}\right) = 0 \text{ in } \Gamma_F, \quad (3)$$

$$\frac{\partial\eta}{\partial t} + U\frac{\partial\eta}{\partial x} = \frac{\partial\phi_w}{\partial y} \text{ in } \Gamma_F. \quad (4)$$

to incorporate the boundaries Γ_I and Γ_D , the Equations (3) and (4) are combined as:

$$\frac{\partial^2\phi_w}{\partial t^2} + 2U\frac{\partial^2\phi_w}{\partial t\partial x} + U^2\frac{\partial^2\phi_w}{\partial x^2} = -g\frac{\partial\phi_w}{\partial y}, \quad (5)$$

by adopting the theoretical linear velocity potential in the absence of current, that is written as:

$$\phi_w = \frac{ag}{\omega} \frac{\cosh(k(y+h))}{\cosh(kh)} \cos(\omega t - kx), \quad (6)$$

and using the second derivatives with respect to x and t of Equation (6), it is verified that at the free surface in absence of current, we have:

$$g\frac{\partial\phi_w}{\partial y} = -c_{kh}^2\frac{\partial^2\phi_w}{\partial x^2}, \quad (7)$$

using Equations (5) and (7), the equation governing the free surface in the presence of current becomes:

$$\frac{\partial^2\phi_w}{\partial t^2} + 2U\frac{\partial^2\phi_w}{\partial t\partial x} + (U^2 - c_{kh}^2)\frac{\partial^2\phi_w}{\partial x^2} = 0, \quad (8)$$

the upstream Γ_I and downstream Γ_D conditions are incorporated in the formulation of equations governing the problem by factorizing the Equation (8) as:

$$\left(\frac{\partial}{\partial t} + c_- \frac{\partial}{\partial x}\right)\left(\frac{\partial}{\partial t} + c_+ \frac{\partial}{\partial x}\right)\phi_w = 0, \quad (9)$$

Then, the generating absorbing boundary conditions (GABC's) are elaborated for the wave-current interactions using the method of characteristic as:

- at the downstream Γ_D boundary, it reads:

$$\left(\frac{\partial}{\partial t} + c_- \frac{\partial}{\partial x}\right)\phi_w = 0 \text{ in } \Gamma_D \quad (10)$$

- at the upstream Γ_I boundary, it reads:

$$\left(\frac{\partial}{\partial t} + c_+ \frac{\partial}{\partial x}\right)\phi_w = WC \text{ in } \Gamma_I \quad (11)$$

by considering that the velocity potential is harmonic and symmetric, such as [10]:

$$\phi_w(x, y, t) = \phi(x, y)e^{i\omega t}, \quad (12)$$

the system of equations governing the problem to resolve is written as:

$$\Delta\phi = 0 \text{ in } \Omega, \quad (13)$$

$$\frac{\partial \phi}{\partial y} = 0 \text{ in } \Gamma_B, \quad (14)$$

$$(U^2 - c_{kh}^2) \frac{\partial^2 \phi}{\partial x^2} + 2i\omega U \frac{\partial \phi}{\partial x} - \omega^2 \phi = 0 \text{ in } \Gamma_F, \quad (15)$$

$$c_- \frac{\partial \phi}{\partial x} + i\omega \phi = 0 \text{ in } \Gamma_D, \quad (16)$$

$$c_+ \frac{\partial \phi}{\partial x} + i\omega \phi = WC \text{ in } \Gamma_I. \quad (17)$$

where WC stands for the incoming waves and currents from the upstream, η is free-surface elevation, g is acceleration attributable to gravity, U is uniform current and ϕ_w is unsteady wave potential

The dispersion relation in the presence of current is expressed as:

- In the case where the current and the direction of propagation of waves are the same, ω and k^- are associated by the following dispersion relation, it reads:

$$(\omega - Uk^-)^2 = gk^- \tanh(k^-h) \quad (18)$$

- In the case where the current are in opposite direction of propagation of waves, ω and k^+ are associated by the following dispersion relation, it reads:

$$(\omega + Uk^+)^2 = gk^+ \tanh(k^+h) \quad (19)$$

where k^- is the wave number of the wave that propagates in the same direction of the current, and k^+ is the wave number of the wave that propagates in inverse direction of the current, c_- and c_+ respectively, are the wave speed at the upstream and downstream, that are expressed respectively as $c_- \equiv U - c_{kh}$, and $c_+ \equiv U + c_{kh}$, by supposing that the current is subcritical $-c_{kh} < U < c_{kh}$, where $c_{kh} = \sqrt{\frac{g h \tanh(kh)}{kh}}$ is the wave celerity in the absence of current. For sake of clarity, when $U = 0$ m/s Equation (9) is the same as the Orlansky condition [22].

3. Numerical Formulation

In this section, we propose the method of fundamental solutions [10–13] (MFS) to resolve the equations governing the linear problem of wave-current interactions, by the implementation of the fundamental solution of 2D Laplace equation that is expressed as:

$$\phi_i(x, y) = \sum_{j=1}^{N_s} \beta_j G(r_{ij}) \quad (20)$$

by applying the boundary conditions, the linear system to resolve is formed as:

$$[A] \left\{ \begin{array}{c} \beta_1 \\ \beta_2 \\ \vdots \\ \vdots \\ \beta_{n-1} \\ \beta_{N_s} \end{array} \right\} = \{S\} \quad (21)$$

more explicitly, the Equation (19) is written as:

$$\begin{bmatrix} A_I \\ A_B \end{bmatrix} \begin{Bmatrix} \beta_1 \\ \beta_2 \\ \vdots \\ \vdots \\ \beta_{n-1} \\ \beta_{N_s} \end{Bmatrix} = \begin{Bmatrix} 0 \\ S_B \end{Bmatrix} \quad (22)$$

where $G(r_{ij}) = \frac{-1}{2\pi} \ln(r_{ij})$ is the Green's function, and $r_{ij} = \sqrt{(x_i - \gamma_j)^2 + (y_i - \delta_j)^2}$ is the distance between field points ($\vec{x}_i = (x_i, y_i)$: black symbols) and source points ($\vec{s}_j = (\gamma_j, \delta_j)$: green symbols), $((x_c, y_c)$: red symbols) are the location of boundary field points, β_j is unknown the coefficients to determine. Even more, the component $[A]$ is the representation of the fundamental solutions, and includes the combination of boundary conditions, $\{S\}$ is the second member.

Precisely, A_I and A_B are respectively the matrix for the inner and boundary collocation points. For sake of clarity, A_I is a $N_I \times N_s$ matrix for the inner collocation points, A_B is a $N_B \times N_s$ matrix for the boundary collocation points, and S_B is a vector of second member data associated with N_s number of source points.

The computational domain is illustrated in the Figure 2, by adopting a distance b to be free from singularities, which are coming from the collocation of boundary conditions. For sake of clarity, the source points are expressed as:

$$S \rightarrow (\gamma_j, \delta_j) = \begin{cases} \gamma_j = x_c + b \left(x_c - \frac{L}{2} \right) \\ \delta_j = y_c + b \left(y_c - \frac{H}{2} \right) \end{cases} \quad (23)$$

By inverting the linear system (22) the coefficients β_j are determined. Next, $\phi(x, y)$ is the fundamental solutions of 2D Laplace equation that is obtained immediately by adopting the linear combination of fundamental solutions. Further, $\phi_w(x, y, t)$ the velocity potential is deducted automatically from Equation (12), and then the free surface water waves elevation $\eta(x, t)$ is obtained from Equation (3).

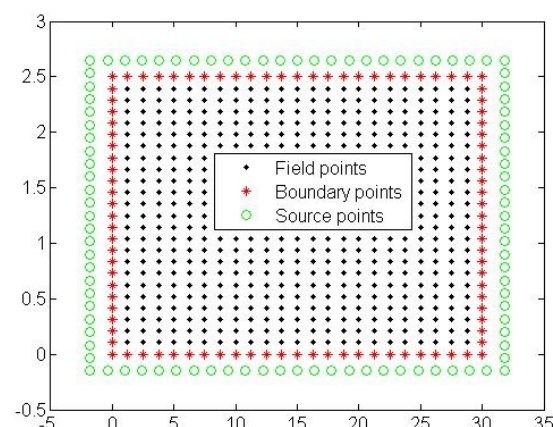


Figure 2. Distribution of field points and boundary points.

4. Results and Discussions

4.1. Validation Test

In this subsection, we will compare the numerical elevations of free surface water waves with analytical ones, for different cases of current (coplanar current, without current, and opposing current), in a computational domain (Figure 1) with constant depth $h = 2.5$ m,

length $L = 15$ m, wave amplitude $a = 0.01$ m and wave period $T = 2.06$ s, where the linear waves and uniform currents are in interactions along the x -direction using the CABCs. The validation tests are described in the Figure 3 along the numerical wave tank for different total nodes numbers, and also for different locations of source points.

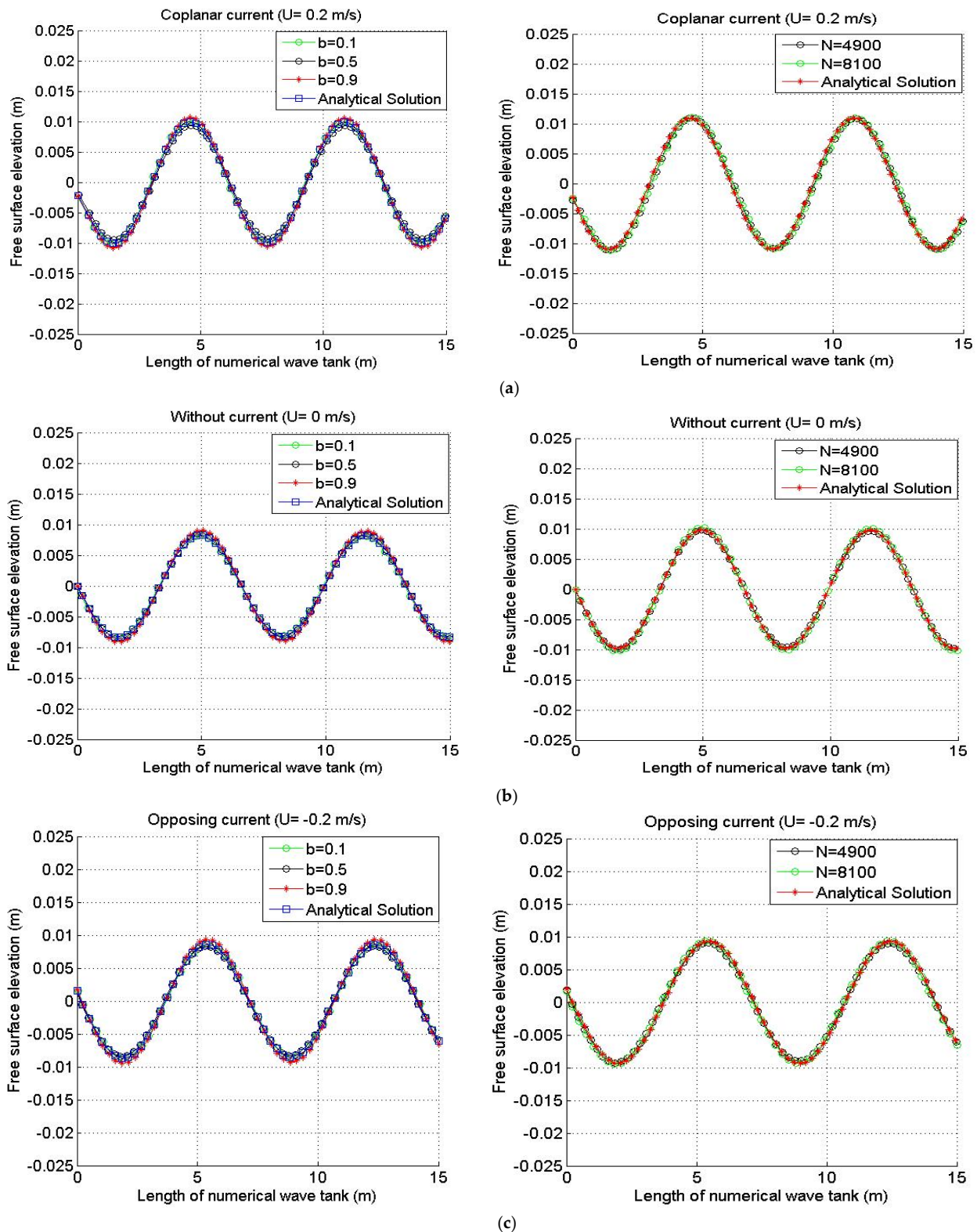


Figure 3. Free surface elevation for different locations of source points (left) and for different total nodes numbers (right) in the case of: (a) Coplanar current, (b) Without current, (c) Opposing current.

The outcomes presented in Figure 3 have shown to be stable and reliable for different total nodes numbers, and for different locations of source points, which confirm the validity of GABCs using the method of fundamental solutions (MFS). For sake of clarity, the next subsection will describe with great extent the stability analysis associated with different total nodes number, locations of source points, for different cases of currents and different water depths.

4.2. Stability Analysis

In this part of this section, to make sure of stability of the present model to treat the wave-current interactions using the CABCs, the root mean-square errors (RMSE) applied to the free surface water waves elevations for different cases of current, are evaluated in the Table 1 for different total nodes numbers, and for different locations of source points. Further, to check the stability of GABCs applied to the wave wave-current interactions, we have evaluate in the Table 2 the RMSE of free surface water waves elevations for different water depths, and for different cases of currents (coplanar current, without current, and opposing current) by fixing $b = 0.1$ m and the total nodes number $N = 4900$. The RMSE presents an index of accuracy measures that defined as:

$$\text{RMSE} \equiv \sqrt{\frac{\sum_{i=1}^N (\text{numerical result} - \text{exact solution})_i^2}{N}} \quad (24)$$

where the exact solutions is written as:

$$\eta(x, t) = \frac{1}{\left(1 - \frac{k^\pm U}{\omega}\right)} \text{asin}(\omega t - k^\pm x) - \frac{U^2}{2g} \quad (25)$$

Table 1. RMSE of free surface water waves elevations for different total nodes number, and for different locations of source points, and for different cases of currents.

	b	$N = 400$	$N = 625$	$N = 1600$	$N = 4900$	$N = 6400$	$N = 8100$
Coplanar current $(U = 0.2 \text{ m/s})$	0.1	1.8×10^{-3}	1.5×10^{-4}	1.7×10^{-4}	1.2×10^{-4}	1.4×10^{-4}	0.9×10^{-4}
	0.3	1.9×10^{-2}	1.6×10^{-3}	1.3×10^{-3}	1.8×10^{-4}	1.6×10^{-4}	1.2×10^{-4}
	0.6	21×10^{-2}	1.5×10^{-2}	1.4×10^{-2}	1.9×10^{-3}	1.6×10^{-3}	1.8×10^{-3}
	0.9	2.1×10^{-2}	1.8×10^{-2}	1.6×10^{-3}	1.4×10^{-3}	1.6×10^{-3}	1.3×10^{-3}
Without current $U = 0 \text{ m/s}$	0.1	1.9×10^{-3}	1.6×10^{-4}	1.6×10^{-4}	1.4×10^{-4}	1.8×10^{-4}	1.2×10^{-4}
	0.3	1.7×10^{-2}	1.8×10^{-3}	1.5×10^{-3}	1.7×10^{-4}	1.9×10^{-4}	1.6×10^{-4}
	0.6	2.1×10^{-2}	1.9×10^{-2}	1.7×10^{-2}	2×10^{-3}	1.8×10^{-3}	1.9×10^{-3}
	0.9	2.2×10^{-2}	1.8×10^{-2}	1.7×10^{-3}	1.8×10^{-3}	1.9×10^{-3}	1.5×10^{-3}
Opposing current $U = -0.2 \text{ m/s}$	0.1	1.6×10^{-4}	1.3×10^{-4}	1.4×10^{-4}	1.3×10^{-4}	1.6×10^{-4}	1×10^{-4}
	0.3	1.8×10^{-4}	1.7×10^{-4}	1.5×10^{-4}	1.7×10^{-4}	1.9×10^{-4}	1.3×10^{-4}
	0.6	1.8×10^{-3}	1.6×10^{-3}	1.4×10^{-3}	1.9×10^{-3}	1.5×10^{-3}	1.5×10^{-3}
	0.9	1.9×10^{-3}	1.7×10^{-3}	1.5×10^{-3}	1.2×10^{-3}	1.6×10^{-3}	1.4×10^{-3}

Table 2. The RMSE of free surface water waves elevations for different water depths, and for different cases of currents.

	$h = 0.5 \text{ m}$	$h = 2.5 \text{ m}$	$h = 5 \text{ m}$
Coplanar current $(U = 0.2 \text{ m/s})$	1.6×10^{-3}	1.2×10^{-4}	1.8×10^{-4}
Without current $(U = 0 \text{ m/s})$	1.9×10^{-2}	1.4×10^{-3}	1.6×10^{-3}
Opposing current $(U = -0.2 \text{ m/s})$	1.7×10^{-3}	1.3×10^{-4}	1.7×10^{-4}

The results illustrated in Table 1 demonstrate that MFS has strong capability to treat the wave-current interactions for different cases of current using the GABCs. Further, the MFS method has been proven a strong stability for different total nodes numbers. Furthermore, our numerical experiments have shown that the MFS method has a good agreement with analytical solution when the value of special parameter b (that describes the locations of source points) is beyond the range [0.1–0.9 m], outside of this range the MFS happened to be instable to treat the waves current interactions. Further, in the Table 2 the RMSE of the free surface water waves elevations for different water depths (shallow, intermediate, and deep water) has proven the stability of the GABCs for different water depths. Furthermore, the outcomes illustrated in the Table 2 have shown that the GABCs in perform better than the Orlandi condition.

5. Conclusions and Perspectives

In this research work, the stability of MFS for the use case of wave-current interactions for different aspect of currents (coplanar current, without current, and opposing current) using the GABCs is deeply discussed. Further, the outcomes of this paper have proven that the MFS method is reliable and stable for the special parameter b within the interval of [0.1–0.9 m], outside of this range the MFS method appears instable. Besides, the MFS method has demonstrated strong efficiency to treat the wave-current interactions for different total nodes number, which confirm the power of the MFS for the use of wave-current interactions using the GABCs approach. Furthermore, the accuracy and stability of the present purpose for different water depths (shallow, intermediate, and deep water) have been also studied, and then the results have shown that the GABCs is stable and accurate and perform better than the Orlandi condition. As perspective, we endeavor to study the wave-current structures interactions using the GABCs approach to carefully measure the reflection and transmission coefficients for different aspect of currents.

Author Contributions: Conceptualization, M.L., D.D., K.K. and D.N.; methodology, M.L., D.D., K.K. and D.N.; software, M.L., D.D., K.K. and D.N.; validation, M.L., D.D., K.K. and D.N.; formal analysis, M.L., D.D., K.K. and D.N.; investigation, M.L., D.D., K.K. and D.N.; resources, M.L., D.D., K.K. and D.N.; data curation, M.L., D.D., K.K. and D.N.; writing—original draft preparation, M.L., D.D., K.K. and D.N.; writing—review and editing, M.L., D.D., K.K. and D.N.; visualization, M.L., D.D., K.K. and D.N.; supervision, M.L., D.D., K.K. and D.N.; project administration, M.L., D.D., K.K. and D.N.; funding acquisition, M.L., D.D., K.K. and D.N. All authors have read and agreed to the published version of the manuscript.

Funding: The work of DD has been supported by the French National Research Agency, through the Investments for Future Program (ref. ANR-18-EURE-0016—Solar Academy).

Institutional Review Board Statement: Not applicable.

Informed Consent Statement: Not applicable.

Data Availability Statement: Not applicable.

Acknowledgments: The Authors would like to express their gratitude to the Referees who helped us to improve our manuscript quality.

Conflicts of Interest: The authors declare no conflict of interest.

Abbreviations

The following abbreviations are used in this manuscript:

MFS	Method of fundamental solutions
GABCs	Generating absorbing boundary conditions
NWT	Numerical wave tank
RMSE	Root mean square error

References

1. Manolidis, M.; Orzech, M.; Simeonov, J. Rogue wave formation in adverse ocean current gradients. *J. Mar. Sci. Eng.* **2019**, *7*, 26. [[CrossRef](#)]
2. Chen, L.; Ning, D.; Teng, B.; Zhao, M. Numerical and experimental investigation of nonlinear wave-current propagation over a submerged breakwater. *J. Eng. Mech.* **2019**, *143*, 9. [[CrossRef](#)]
3. Lin, H.; Ning, D.; Zou, Q.; Teng, B. Current effects on nonlinear wave scattering by a submerged plate. *J. Waterway Port Coast. Ocean Eng.* **2014**, *140*, 5. [[CrossRef](#)]
4. Gholamipour, M.; Ghiasi, M. A meshless numerical wave tank for simulation of fully nonlinear wave-wave and wave-current interactions. *J. Eng. Math.* **2019**, *119*, 115–133. [[CrossRef](#)]
5. He, M.; Gao, X.; Xu, W. Numerical simulation of wave-current interaction using the SPH method. *J. Hydrodyn.* **2018**, *3*, 535–538. [[CrossRef](#)]
6. Ni, X.; Feng, W.; Huang, S. An SPH wave-current flume using open boundary conditions. *J. Hydrodyn.* **2019**, *179*, 604–612. [[CrossRef](#)]
7. Zhang, J.; Zhang, Y.; Jeng, D.S.; Liu, P.; Zhang, C. Numerical simulation of wave-current interaction using a RANS solver. *Ocean Eng.* **2014**, *75*, 157–164. [[CrossRef](#)]
8. Fan, M.; Ch, N.; Šarler, B. Numerical solutions of waves-current interactions by generalized finite difference method. *Eng. Anal. Bound. Elem.* **2019**, *100*, 150–163. [[CrossRef](#)]
9. Zhang, T.; Ren, F.; Yang, Z. Application of generalized finite difference method to propagation of nonlinear water waves in numerical wave flume. *Ocean Eng.* **2016**, *123*, 278–290. [[CrossRef](#)]
10. Loukili, M.; Mordane, S. New numerical investigation using meshless methods applied to the linear free surface water waves. *Adv. Intell. Syst. Comput.* **2019**, *765*, 337–345.
11. Loukili, M.; Mordane, S. Numerical Analysis of an Absorbing Boundary Condition Applied to the Free Surface Water Waves Using the Method of Fundamental Solutions. In Proceedings of the 8th International Conference on Modeling Simulation and Applied Optimization (ICMSAO), Manama, Bahrain, 15–17 April 2019.
12. Loukili, M.; Kotrasova, K.; Mouhid, M. Computerized Decision Aid Applied to Meshless Method for the Use Case: Wave-Structure Interactions. In Proceedings of the 2020 International Conference on Decision Aid Sciences and Application (DASA), Sakheer, Bahrain, 8–9 November 2020.
13. Loukili, M.; El Aarabi, L.; Mordane, S. Computation of nonlinear free-surface flows using the method of fundamental solutions. *Adv. Intell. Syst. Comput.* **2019**, *763*, 420–430.
14. Kupradze, D.; Aleksidze, M. The method of functional equations for the approximate solution of certain boundary value problem. *Zh. Vych. Mat.* **1964**, *4*, 82–126. [[CrossRef](#)]
15. Bogomolny, A. Fundamental solutions method for elliptic boundary value problems. *SIAM J. Numer. Anal.* **1985**, *22*, 644–669. [[CrossRef](#)]
16. Golberg, M.A.; Chen, C.S. The method of fundamental solutions for potential, Helmholtz and diffusion problems. In *Boundary Integral Methods Numerical and Mathematical Aspects*; Computational Mechanics Publications: Southampton, UK, 1998.
17. Loukili, M.; Mordane, S. New contribution to stokes equations. *Adv. Appl. Fluid Mech.* **2017**, *20*, 107–116. [[CrossRef](#)]
18. Young, D.L.; Lin, Y.C.; Fan, C.M. The method of fundamental solutions for solving incompressible Navier–Stokes problems. *Eng. Anal. Bound. Elem.* **2009**, *33*, 1031–1044. [[CrossRef](#)]
19. Karageorghis, A.; Fairweather, G. The method of fundamental solutions for the numerical solution of the biharmonic equation. *J. Comput. Phys.* **1987**, *69*, 434–459. [[CrossRef](#)]
20. Xiao, L.F.; Yang, J.M.; Peng, T. A meshless numerical wave tank for simulation of nonlinear irregular waves in shallow water. *International journal for numerical methods in fluids.* **2009**, *61*, 165–184.
21. Wu, N.J.; Tsay, T.K.; Young, D.L. Computation of nonlinear free-surface flows by a meshless numerical method. *J. Waterway Port Coast. Ocean Eng.* **2008**, *134*, 97–103. [[CrossRef](#)]
22. Orlansky, I. A simple boundary condition for unbonded hyperbolic flows. *J. Comput. Phys.* **1976**, *21*, 251–269. [[CrossRef](#)]